Thermochimica Acta, 241 (1994) 131–156
Elsevier Science B.V., Amsterdam
SSDI 0040-6031(94)01729-Z

Molecular thermodynamics of the denaturation of lysozyme

A. Braibanti* and E. Fisicaro

Institute of Applied Physical Chemistry, University of Parma, I-43100 Parma, Italy

(Received 11 October 1993; accepted 22 January 1994)

Abstract

The macromolecular system where denaturation takes place, is considered from a molecular thermodynamic point of view as a convolution of a grand canonical ensemble, *gce* and a canonical ensemble *ce*. The former corresponds to the solute, the latter to the solvent.

The properties of this system can be represented by a convoluted partition function obtained by the product of a grand canonical partition function Z_N, and a canonical partition function, ζ_W. If the experimental equilibrium constant, $K_{den} = [D_{hyd}]/[N]$ is substituted for Z_N and $[W]^{nw}$ for ζ_W, the convoluted partition function is $K_0 = K_{den}[W]^{nw}$, where [W] is the concentration of the solvent in the bulk and n_W is the number of water molecules involved in the reaction. According to this model, by calculating the derivative $\partial \ln K_{den}/\partial(1/T)$, values of the denaturation enthalpy ΔH_{den} should be obtained which are a linear function of the absolute temperature. The slope of the straight line $\Delta H_{den} = f(T)$ is dependent upon n_W. The experimental equilibrium constant conforms to the model.

The apparent isobaric heat capacity, $C_{p,app}$ of the solute is calculated by double mixed derivation of $\ln Z_N$ with respect to $\ln[W]^{-nw}$ and $\ln T$. By integration between two temperatures, as in DSC experiments, the apparent isobaric heat capacity yields the apparent enthalpy ΔH_{den} of the denaturation process. The enthalpy thus calculated ΔH_{den} should be a linear function of the denaturation temperature T_m in agreement with the denaturation enthalpy obtained by deriving the logarithm of the denaturation equilibrium constant. In fact, the heat supplied is comprehensive of the enthalpy due to the change of the conformation of the protein from native to denatured ΔH_{conf}, of the hydration enthalpy, ΔH_{hyd}, and of a term, $n_W C_{p,W} T_m$, due to the heat absorbed by n_W water molecules involved in the reaction

$$\Delta H_{den} = \Delta H_{conf} + \Delta H_{hyd} + n_W C_{p,W} T_m$$

The hen egg white lysozyme (mol. wt. 14 100 Da) changes the denaturation enthalpy, and correspondingly the denaturation temperature T_m by changing the pH or the concentration of denaturant. The influence of pH is related to changes in the structure of the solvent rather than to an actual reaction process. In accordance with this hypothesis, the dependence of the denaturation enthalpy either from $\ln T$ or from pH or from denaturant concentration follows the same law. Values of ΔH_{den} for hen egg white lysozyme plotted as the function of temperature give a unique straight line with slope corresponding to $n_W = 88.9$ water molecules.

The same treatment has been applied to the denaturation enthalpy for wild lysozyme of the bacteriophage T4 (mol. wt. 18 700 Da), as determined in DSC experiments. The slope of

* Corresponding author.

the line yields $n_W = 122.0$ water molecules. The difference in the number of water molecules is related to the different size of the macromolecules and probably to the proportional number of hydrophobic residues. The number of water molecules changes with different substituents. Mutants of wild lysozyme appear to involve $n_W = 131.4$ and 139.8 for T157A and R96H, respectively. These numbers are in agreement with the increased hydrophobic character of the entering groups.

The process seems to be related to the formation of a cage of water molecules around the denatured protein.

LIST OF SYMBOLS

[A]	concentration of free A
AH_i	species
ce	canonical ensemble
$C_{p,app}$	apparent isobaric heat capacity
$C_{p,W}$	molar isobaric heat capacity of water
D	denatured protein
D_{hyd}	hydrated denatured protein
$\exp(-\Delta G_i/RT)$	joint probability, level i
$\exp(-\Delta H_i/RT)$	enthalpy probability factor, level i
$\exp(\Delta S_H/R)$	enthalpy-equivalent entropy factor
$\exp(\Delta S_i/R)$	entropy probability factor, level i
$\exp(\Delta S^{\ominus}/R)$	standard entropy factor
$(gc^{\star}c)\boldsymbol{e}$	convoluted ensemble
gce	grand canonical ensemble
[GuHCl]	concentration of guanidium chloride
ΔG_{den}	denaturation free energy
$\Delta \boldsymbol{G}^{\ominus}_{den}$	free energy change vector
ΔG_i	free energy difference, level i
$\Delta G^{\ominus}/RT$	standard free energy change
$\Delta \boldsymbol{H}_{conf}$	conformational enthalpy vector
$\Delta \boldsymbol{H}_{den}$	denaturation enthalpy vector
$\Delta \boldsymbol{H}_{hyd}$	hydration enthalpy vector
ΔH_i	enthalpy difference between level i and level 0
ΔH_W	enthalpy term due to water
$\Delta \boldsymbol{H}_W$	water enthalpy vector
$\Delta \boldsymbol{H}_0$	reaction enthalpy vector
ΔH^0	extrapolated enthalpy
$\boldsymbol{i}, \boldsymbol{j}, \boldsymbol{k}$	unitary vectors
K	equilibrium constant (saturation partition function)
K_{conf}	conformational transient constant from N to D
K_{den}	denaturation constant from N to D_{hyd} state
K_{hyd}	hydration constant
K_0	total constant (= convoluted partition function)
level i	ith complex MA_i or MH_i or AH_j or XA_i of a set

[M]	concentration of free M
MA_i	species
MH_i	species
$\langle n \rangle$	formation function or binding isotherm
n_W	number of water molecules
N	native protein
[P]	total protein
R	gas constant
sublevel j	jth sublevel of ith complex
$\Delta \boldsymbol{S}_{conf}$	conformational entropy vector
$\Delta S_d/R$	relative dilution of the ligand
ΔS_{den}	denaturation entropy
ΔS_i	intrinsic entropy difference of the reaction, level i
ΔS_W	entropic contribution of n_W water molecules
$\Delta \boldsymbol{S}^{\ominus}$	standard entropy vector
$\Delta \boldsymbol{S}^{\ominus}_{den}$	denaturation entropy vector
$\Delta \boldsymbol{S}^{\ominus}_{W}$	vector in thermodynamic space
$\Delta \boldsymbol{W}^{\ominus}_{W}$	water enthalpy vector
T	absolute temperature/K
TED	thermal equivalent dilution
$x = \exp(\Delta S/R)$	axis of probability space
$x = (\Delta S/R)$	axis of affinity thermodynamic space
$x\boldsymbol{i} + y\boldsymbol{j} = z\boldsymbol{k}^*$	coplanar vectors
X	free receptor
XA_i	species
$y = \exp(-\Delta H/RT)$	axis of probability space
$y = (-\Delta H/RT)$	axis of affinity thermodynamic space
$z^* = \exp(-\Delta G^{\ominus}/RT)$	coplanar axis of probability space
$z^* = (-\Delta G^{\ominus}/RT)$	coplanar axis of affinity thermodynamic space
Z_M	excess grand canonical partition function referred to M
Z_N	excess grand canonical partition referred to native protein
$Z_N\zeta_W$	convoluted partition function
Z_X	excess grand canonical partition function referred to X
$Z^{\ominus}_X$	excess partition function in standard state
$Z^*_X = Z_X\zeta_i$	convoluted partition function

Greek letters

$\alpha_{c,D}$	cold fraction of denatured protein
α_D	fraction of denatured protein
α_N	fraction of native protein

ζ_i	canonical partition function of species i
ζ_W	canonical partition function of water, W
κ	dissociation constant referred to T
Ξ_M	grand canonical partition function referred to M

INTRODUCTION

In previous articles [1–14], we have analysed the application of the partition function method to the study of multiple equilibria in solutions of macromolecules. The equilibrium concentrations can be determined by potentiometry, dialysis, spectrophotometry, calorimetry, etc., under different ligand/macromolecule ratios. Alternatively, calorimetric determinations by isothermal, isoperibol, or differential scanning calorimetry, produce further thermodynamic information such as enthalpy and heat capacity of the system in equilibrium.

It has been shown [9, 10] how every enthalpy change is paralleled by an equivalent entropy change whereby the former can be evaluated and vice versa. The van't Hoff equation exploits this equivalence to get information concerning the enthalpy change of a reaction from the equilibrium concentrations of the same reaction at different temperatures, without any direct calorimetric determination whatsoever.

The chemical systems are considered in general as the tokens in the experimental field, of grand canonical ensembles, *gce* of statistical thermodynamics, open to the exchange of heat and matter. If no chemical reaction is taking place, however, the system can be represented by a canonical ensemble, *ce* open to exchange of heat and invariant with respect to the concentration. The properties of each ensemble are represented by means of the corresponding partition function.

The systems where the reaction is taking place in the presence of excess of solvent can be referred to as a convoluted ensemble, $(gc^{\star}c)e$ resulting from the convolution of a grand canonical ensemble, representing the reaction with a canonical ensemble, *ce* representing the solvent. The thermodynamic properties of the convoluted ensemble are expressed by the product of grand canonical and canonical partition functions. The denaturation of proteins takes place in the presence of excess of solvent. Therefore, the description of the denaturation process by means of convoluted partition functions seems appropriate.

The treatment will be applied to the analysis of the denaturation of different types of lysozyme for which a linear dependence of the denaturation enthalpy ΔH_{den} upon the denaturation temperature T_m has been found [15–20]. Further developments of the model are needed to cope with systems where the function $\Delta H_{den} = f(T_m)$ is not linear as for example in hen egg white lysozyme in the presence of sarcosine [20] or where the behaviour is pH dependent as in chymotropysinogen or in ribonuclease [21–23].

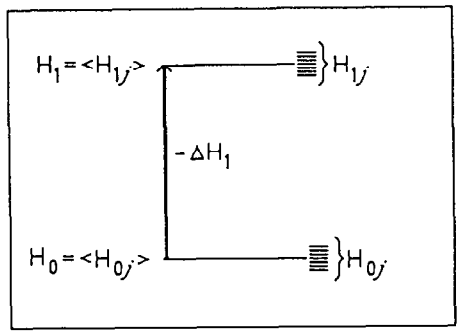

Fig. 1. Enthalpy levels H_i and enthalpy sublevels H_j in grand canonical ensemble. The same distribution as for sublevel j holds for a canonical ensemble.

PARTITION FUNCTIONS AND ENSEMBLES

The partition function method consists in finding the relationship of the experimental measurements of concentrations, dilution and heat to the probability of occurrence of a chemical or physicochemical process. Following Poland [24], the process is seen with reference to a quantized energy level model (Fig. 1) representing the molecular element of a molar statistical ensemble. Each level of the model corresponds to a single complex MA_i, or MH_i, AH_i, XA_i, etc., that can be transformed into another one $MH_{i\pm1}$, or $MH_{i\pm1}$, $AH_{i\pm1}$, $XA_{i\pm1}$, etc., by changing either the ligand concentration or the temperature.

Within each level i, the complex occupies sets of sublevels j and the redistribution among these sublevels takes place only by addition or subtraction of heat.

The distribution of the species among the different levels i of *gce* is calculated by means of the excess grand canonical partition function, Z_M or the grand canonical partition function, $\Xi_M = [M]Z_M$. Each level is characterized by a number of cells. The number of cells (or states) represents the degeneracy of the level and corresponds to dilution or equivalent dilution in the experimental chemical domain [10].

Any level i is separated from the fundamental level by the enthalpy difference ΔH_i. The number of accessible cells (or states) within each level is related to the entropy of the level (Fig. 2). The number of the accessible (empty) cells can be varied by changing the dilution [10]. Starting from an initial state where free M and free A are mixed (Fig. 2(a)), the binding of M and A to form MA is equivalent to increasing the number of the empty accessible cells, and hence to dilute free A (Fig. 2(b)). This yields an increase of the entropy of the system. The increase of the number of empty cells is proportional to the enthalpy difference ΔH_i. Actually, a further increase or decrease of the number of empty cells takes place due to the intrinsic entropy difference of the reaction, ΔS_i. On the whole, the total

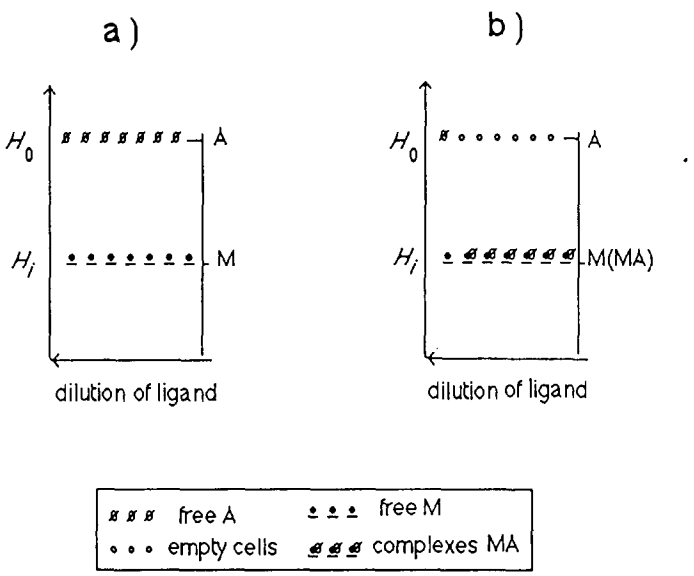

Fig. 2. Enthalpy levels and dilution of ligand: (a) free A is added to the solution occupying the upper level; (b) excess of A is bound to M, thus diluting A.

dilution of the ligand is proportional to the affinity of the ligand A for the receptor M and is comprehensive of both enthalpy and entropy contributions.

The probability of transitions between levels is expressed by the joint probability

$$\exp(-\Delta G_i/RT) = \exp(-\Delta H_i/RT)\exp(\Delta S_i/R) \quad (1)$$

The distribution of the population among the whole set of levels is given by the excess partition function

$$Z_X = \sum_i [XA_i]/[X] \quad (2)$$

where the free receptor concentration [X] is taken as the normalizing reference state and A is a ligand.

The model is well suited to describe the effect either of concentration or temperature on the distribution of the species. The various mathematical expressions of the logarithms of partition functions Z_X, or equilibrium constants or kinetic constants as the function of concentration or temperature or reciprocal temperature are connected to the partition of species over the different levels of the model. The mathematical expressions depend on the partition function appropriate to the system. The experimental observations corresponding in general to derivatives of the functions represent evaluations of changes in the partition of the species.

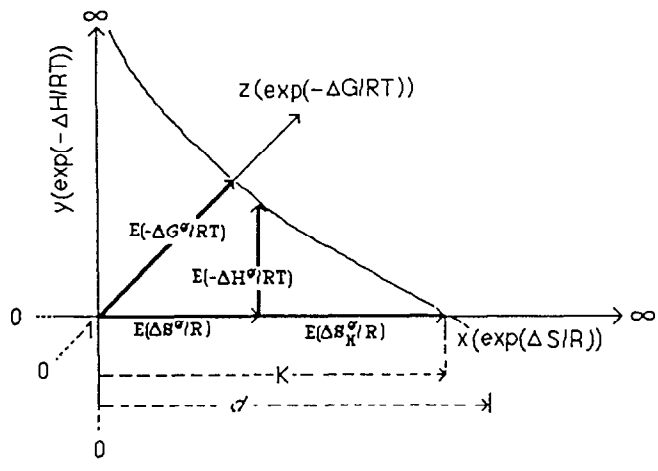

Fig. 3. Probability space. E( ) stands for exp( ), for the sake of brevity. K is the equilibrium constant, d is the dilution.

The partition function is related to the probability of transition and to the standard free energy change by

$$Z_X^{\ominus} = \exp(-\Delta G^{\ominus}/RT) \tag{3}$$

which can be factorized into enthalpy probability and entropy probability

$$\exp(-\Delta G^{\ominus}/RT) = \exp(-\Delta H^{\ominus}/RT)\exp(\Delta S^{\ominus}/R) \tag{4}$$

The joined probability can be represented in the probability space where the axes are $x = \exp(\Delta S/R)$ and $y = \exp(-\Delta H/RT)$ (Fig. 3). The joined probability $z^* = \exp(-\Delta G^{\ominus}/RT)$ is represented in the auxiliary coplanar axis z^*. The starred coordinate indicates that for geometrical conditions of the axes in one plane, the scale along the auxiliary axis is multiplied by $1.414 = 2\cos 45°$.

The geometrical representation is useful to put in evidence several relationships between thermodynamic functions and experimental observations. A useful step has been the identification of $x = \exp(\Delta S/R)$ with the dilution axis related to the number of accessible cells of the level model (see Fig. 2). Partition functions and equilibrium constants are also evaluated along x. It is important to note that the enthalpy factor $\exp(-\Delta H^{\ominus}/RT)$ along the y axis can be evaluated as a corresponding equivalent entropy factor $\exp(\Delta S_H/R)$ along the x axis. In the probability space in fact, the equivalent entropy factor is the hyperbolic projection onto x of $\exp(-\Delta H/RT)$. The equilibrium constant is evaluated along x as the hyperbolic projection of $\exp(-\Delta G^{\ominus}/RT)$ onto x. Thus the equilibrium constant K or the partition function $Z_X^{\ominus}$ comes out to be a total entropic quantity, obtained as the product of the standard entropy factor $\exp(\Delta S^{\ominus}/R)$ and the equivalent entropy factor $\exp(\Delta S_H/R)$.

The partition function depends on the formation constants of the species included in the function itself. In the simple case of the equilibrium $M + A = MA$, the partition function is

$$Z_M = 1 + K[A] \tag{5}$$

Even the equilibrium constant K by itself can be identified with a saturation partition function giving the ratio between the probability of binding A to form MA and the probability of dissociating it [4, 6]. The partition function and the equilibrium constant can be considered as dilutions or reciprocal concentrations and read on the diagrams of the probability space. In this space, the x axis is parallel to the dilution axis, $x \parallel d$.

The probability space can be transformed into the affinity thermodynamic space by taking the logarithms of the probabilities of the eqns. (1–5). In affinity thermodynamic space, the axis representing $\ln K$, $\ln Z_M$, and $\ln d$ is parallel to the x axis (entropy axis).

The thermodynamic space is useful to represent the relations of the thermodynamic functions with the experimental domains of calorimetry and potentiometry. The basic relationship of classical thermodynamics

$$-\Delta G_i/RT = -\Delta H_i/RT + \Delta S_i/R \tag{6}$$

can be represented by vectors in the thermodynamic space, where the scale factor for the starred axis z^* is $0.707 = \cos 45°$ (Fig. 4). An endothermic reaction is represented in this diagram. The equivalent entropy component, $\Delta S_H/R$ is obtained as orthogonal projection of the enthalpy component $-\Delta H/RT$ onto the x axis. Regions of the thermodynamic space where the processes are enthalpy-driven or entropy-driven are clearly identified in this diagram.

It is worth noting that also the Bjerrum formation function or binding isotherm $\langle n \rangle$ giving the average number of ligand bound per mole of receptor

$$\langle n \rangle = \partial \ln Z_M / \partial \ln[A] = \Delta S_d/R \tag{7}$$

represents an evaluation of the relative dilution of the ligand and as such can be identified with an entropy change, $\Delta S_d/R$ and evaluated along x of the thermodynamic space [11].

CONVOLUTED ENSEMBLES

In general the stability constants in solution are determined in the presence of excess of solvent whose concentration is assumed to be constant even if it takes part in the chemical reaction as a ligand. We have shown [12] how in the protonation equilibria of carboxylic acids in aqueous

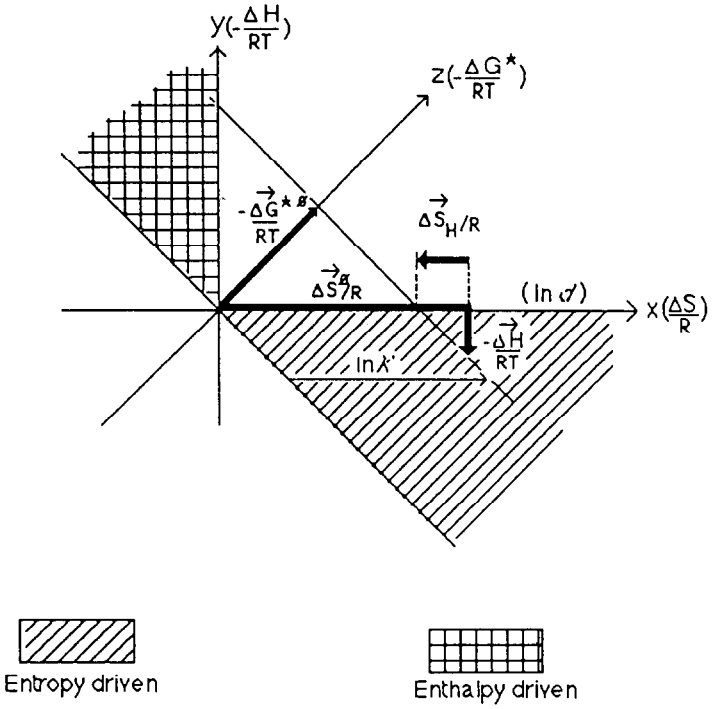

Fig. 4. Thermodynamic space. Enthalpy- and entropy-driven fields. The represented reaction is endothermic and entropy-driven.

solution, the protonation constant lg K determined experimentally is only an apparent constant because it does not include the concentration of water molecules [W] involved in the reaction.

The solvent in these systems can be represented as a canonical ensemble, *ce* whose properties are described by a canonical partition function ζ_i which is independent from the concentration. For *ce*, only moments of the partition function with respect to the variable temperature T or to the variable reciprocal or logarithmic temperature can be measured. The solute in its different species forms a grand canonical ensemble *gce*.

The properties of the ensembles *gce* and *ce* are related to the previously mentioned models consisting of sets of quantized energy levels. The ensembles *gce* and *ce* differ from one another for the extent of the interlevel energy separation. The ensemble *gce* is characterized by enthalpy differences ΔH_i between levels i significantly higher than the differences ΔH_j between sublevels j. The ensemble *ce* consists of a unique level which is the mean of several sublevels j with differences ΔH_j between sublevels. The set of enthalpy levels is similar to that of the sublevels H_j in a single level i (see Fig. 1). A specific partition function can be associated with each component ensemble, namely a grand canonical partition function Z_X with *gce* and a canonical partition function ζ_i with *ce*, respectively.

The protonated and unprotonated species of carboxylic acid in aqueous solution have been represented [12] as a convoluted ensemble $(gc^{\star}c)e$. The protonation process has been described on the basis of a convoluted partition function, $Z_{\mathrm{X}}^{*} = Z_{\mathrm{X}}\zeta_i$ obtained as the product of a grand canonical partition function and a canonical partition function, the last one corresponding to the solvent. The same convolution of partition functions is suited to the interpretation of the solubility of noble gases [13].

The protonation process in the carboxylic acids follows the same scheme in all the acids examined so far. The reaction enthalpy can be decomposed into an exothermic contribution $\Delta H^0 = -45.6 \pm 3.6\ \mathrm{kJ\ mol^{-1}}$ and an endothermic contribution ΔH_{W} which depends on the number of water molecules involved in the reaction. The latter contribution $\Delta H_{\mathrm{W}} = n_{\mathrm{W}} C_{p,\mathrm{W}} T$ is a linear function of the temperature. $C_{p,\mathrm{W}}$ is the molar isobaric heat capacity of water and n_{W} is the number of water molecules involved in the reaction. The number n_{W} comes out to be constant ($n_{\mathrm{W}} = 2.11$) in all the acids examined.

The solubility of noble gases is similarly explained by considering the n_{W} water molecules involved in the formation of a cage around the gas atom. The number of water molecules entering the cage is proportional to the size of the central atom. The number n_{W} ranges from 1.6 for helium to 3.2 for xenon and to 3.9 for radon.

DENATURATION AND van't HOFF EQUATION

The criteria derived from the equivalence of chemical and thermal dilution of the free solvent W and applied to the analysis of the protonation of carboxylic acids or to the solubility of noble gases in water, can be applied to the interpretation of the denaturation of proteins as well. A two step process is assumed [19].

The equilibrium between native N and denatured D states of a protein can be decomposed into two processes. The first process is the conformational transition from N to D state with constant

$$K_{\mathrm{conf}} = [\mathrm{D}]/[\mathrm{N}] \tag{8}$$

This is a highly cooperative process and from a thermodynamic point of view consists in a supply of energy (enthalpy) to the N state which is then transferred as kinetic energy (entropy) to the D state.

The second process is the hydration of the denatured state via the formation of a cavity in the bulk of solvent molecules

$$\mathrm{D} + x\mathrm{W} = \mathrm{DW}_{(x-n_{\mathrm{W}})} + n_{\mathrm{W}}\mathrm{W} \tag{9}$$

with equilibrium constant

$$K_{\mathrm{hyd}} = [\mathrm{D}_{\mathrm{hyd}}][\mathrm{W}]^{n_{\mathrm{W}}}/[\mathrm{D}] \tag{10}$$

where $[D_{hyd}] \gg [D]$ is the concentration of hydrated denatured molecules $DW_{(x-n_W)}$, and [W] is the concentration of water molecules in the bulk. n_W is the number of water molecules of the bulk expelled by D to form a cavity. By substitution of eqn. (8) into eqn. (10), one obtains

$$K_{hyd}K_{conf} = [D_{hyd}][W]^{nw}/[N] = K_0 \tag{11}$$

The denaturation constant K_{den} is

$$K_{den} = [D_{hyd}]/[N] \tag{12}$$

and then by introducing eqns. (10) and (11), eqn. (12) yields

$$K_{den} = K_0[W]^{-nw} \tag{13}$$

K_{den} is related to the grand canonical partition function Z_N by eqn. (22). K_{den} itself can be considered as a grand canonical parition or saturation function [9]. $[W]^{nw}$ is the canonical partition function ζ_W for the solvent and K_0 is the convoluted partition function.

By taking the logarithms, eqn. (13) becomes

$$\ln K_{den} = \ln K_0 - n_W \ln[W] \tag{14}$$

By differentiation with respect to $1/T$, one obtains

$$\partial \ln K_{den}/\partial(1/T) = \partial \ln K_0/\partial(1/T) - n_W \partial \ln[W]/\partial(1/T) \tag{15}$$

By applying the van't Hoff equation to eqn. (15), the denaturation enthalpy ΔH_{den} is obtained

$$-\Delta H_{den}(1/R) = -\Delta H_0(1/R) - n_W \partial \ln[W]/\partial(1/T) \tag{16}$$

The last term of this equation can be transformed into the derivative with respect to $\ln T$

$$-n_W \partial \ln[W]/\partial(1/T) = n_W T \partial \ln[W]/\partial \ln T \tag{17}$$

In canonical ensembles [3], the following equality holds

$$\partial \ln[W]/\partial \ln T = -C_{p,W}/R \tag{18}$$

By introduction of the eqns. (17) and (18) and by division by $-(1/R)$, the denaturation enthalpy of eqn. (16) can be expressed as

$$\Delta H_{den} = \Delta H_0 + n_W T C_{p,W} \tag{19}$$

This means that by plotting the denaturation enthalpy against T, a straight line should be obtained, which is exactly what has been found in the cases examined so far.

DENATURATION FRACTIONS AT DIFFERENT TEMPERATURES

If the concentration of the denatured protein in statistical equilibrium is $[D_{hyd}] \gg [D]$, then the total protein is $[P] = [N] + [D_{hyd}]$ and the fractions of native and denatured protein, respectively are given by

$$\alpha_N = [N]/([N] + [D_{hyd}]) \tag{20}$$

and

$$\alpha_D = [D_{hyd}]/([N] + [D_{hyd}]) \tag{21}$$

The partition function referred to N as the receptor, can be written as

$$Z_N = 1 + K_0[W]^{-n_W} \tag{22}$$

and the fraction α_D

$$\alpha_D = K_0[W]^{-n_W}/(1 + K_0[W]^{-n_W}) \tag{23}$$

can be obtained as derivative of Z_N with respect to $\ln[W]^{-n_W}$

$$\partial \ln Z_N/\partial \ln[W]^{-n_W} = \alpha_D \tag{24}$$

By considering that the molar fraction for a single step reaction is identical with the formation function or binding isotherm and by recalling eqn. (7), the molar fraction can be identified with a charge of entropy of the system, $\Delta S_d/R$. The second derivative of $\ln Z_N$ with respect to $\ln T$ is therefore a change of entropy with temperature and can be calculated as

$$\partial^2 \ln Z_N/\partial(\ln[W]^{-n_W})\partial \ln T = \partial\alpha_D/\partial \ln T \tag{25}$$

The derivative of α_D with respect to $\ln T$ can be calculated explicitly

$$\begin{aligned}\partial\alpha_D/\partial \ln T &= \partial(K_0[W]^{-n_W})/\partial \ln T\{1/(1 + K_0[W]^{-n_W})^2\} \\ &= \{[W]^{-n_W}\partial K_0/\partial \ln T + K_0\partial[W]^{-n_W}/\partial \ln T\} \\ &\quad \times \{1/(1 + K_0[W]^{-n_W})^2\}\end{aligned} \tag{26}$$

The derivative of K_0 with respect to $\ln T$ is

$$\partial K_0/\partial \ln T = K_0(\Delta H_0/RT) \tag{27}$$

By recalling that the solvent is actually a canonical ensemble *ce* [12] for which eqn. (18) holds, the derivative of $[W]^{-n_W}$ with respect to $\ln T$ becomes

$$\partial[W]^{-n_W}/\partial \ln T = +[W]^{-n_W}n_W C_{p,W}/R \tag{28}$$

Equation (26) becomes

$$\begin{aligned}\partial\alpha_D/\partial \ln T &= K_0[W]^{-n_W}(\Delta H_0/RT + n_W C_{p,W}/R)\{1/(1 + K_0[W]^{-n_W})^2\} \\ &= \alpha_D(1 - \alpha_D)(\Delta H_0/RT + n_W C_{p,W}/R)\end{aligned} \tag{29}$$

where the first term within parentheses $\Delta H_0/RT$ refers to the convoluted ensemble $(gc^{\star}c)e$ and the second term $n_W C_{p,W}/R$ to *ce* of the solvent.

The result of these calculations is that the molar fractions of native and denatured states of the macromolecule, respectively, obtained in DSC experiments are the functions of the same factor $(\Delta H_0/RT + n_W C_{p,W}/R)$ affecting the denaturation enthalpy in eqn. (19) had been obtained from equilibrium determinations.

ISOBARIC HEAT CAPACITY

The following equality can be set between molar fraction derivative and apparent isobaric heat capacity because both can be considered as entropy dispersions.

$$|\partial\alpha_D/\partial \ln T| = C_{p,app}/R \tag{30}$$

The right hand side of eqn. (30) is by definition a positive quantity.

The derivative at the left hand side of eqn. (30) is actually a mixed derivative [11]. In fact, the factor $\alpha_D(1-\alpha_D)$ in eqn. (29) can be identified with the buffer capacity of an isothermal titration curve $\alpha_D = f(\ln[W]^{-n_W})_T$

$$\alpha_D(1-\alpha_D) = (\partial\alpha_D/\partial \ln[W]^{-n_W})_T \tag{31}$$

Equation (32) can be rewritten as a product of derivatives of implicit functions

$$(\partial z/\partial x)_y/(\partial z/\partial y)_x = -(\partial y/\partial x)_z$$

$$(\Delta\alpha_D/\partial \ln T)_{[W]} = -(\partial\alpha_D/\partial \ln[W]^{-n_W})_T(\Delta H_0/RT + n_W C_{p,W}/R)_\alpha \tag{32}$$

with variables α_D, $\ln T$ and $[W]^{-n_W}$ bound by implicit relationship

$$C_{p,app}(\alpha_D, \ln T, [W]^{-n_W}) = 0 \tag{33}$$

Equation (30) yields the apparent isobaric heat capacity. We can recall that (see ref. 10, Table 3) the second derivative of the partition function with respect to $\ln T$ is identified with the dispersion of entropy and experimentally measured by the heat capacity of the system. In the same way, the mixed derivative with respect to $\ln T$ and $\ln[W]^{-n_W}$ of eqn. (32) can be identified with dispersion of entropy over sites and over states and experimentally measured by the excess heat capacity of the solute [11].

The application of the relation of implicit functions to the convoluted partition function confirms the validity of eqn. (32), introducing however new insights of the chemical interpretation of the mathematical expressions. In particular, it is important to note that eqn. (32) is coherent with the interpretation of the absolute temperature as a formal analogue of dilution.

By applying the relation of the implicit functions, one can write

$$(\Delta H_0/RT + n_W C_{p,W}/R)_\alpha = \partial \ln[W]^{-n_W}/\partial \ln T \tag{34}$$

which is the explicit expression of the "warm" derivative for reaction (9) in a convoluted ensemble. The first term in parentheses concerns the convoluted ensemble, $(gc^\star c)e$ and the second term the canonical ensemble ce. One can note that apart from the term $n_W C_{p,W}/R$, eqn. (34) is coincident with $\partial(-\Delta G^\ominus/RT)/\partial \ln T$.

We note that by putting $y = (\Delta H_0 RT + n_W C_{p,W}/R)$ in eqn. (34) and by integration, one obtains

$$K_0[W]^{-n_W} = \kappa T^y \tag{35}$$

where K_0 and κ are dissociation constants. This means that we can assimilate the temperature to a kind of reciprocal concentration or thermal equivalent dilution (TED). Under the condition that $y = +1$, the "cold" molar fraction $\alpha_{c,D}$ can be expressed as

$$\alpha_{c,D} = \{K_0[W]^{-n_W}/(1 + K_0[W]^{-n_W}\}_T = \kappa' T/(1 + \kappa' T) \tag{36}$$

where κ' is similar to an equilibrium constant. The molar fractions can be represented in a Bjerrum plane as titration curves (Fig. 5). The different curves are parallel to each other for endothermic reactions, the displacement depending on both the value of the stability constant and concentration units (Fig. 5(a)). If $y = -1$ (exothermic reactions), the slope of the curve is reversed. This means that by differentiation of eqn. (36) with respect to the absissa ($\ln[W]^{-n_W}$ and $\ln T$, respectively) equal or opposite values of the slopes are obtained.

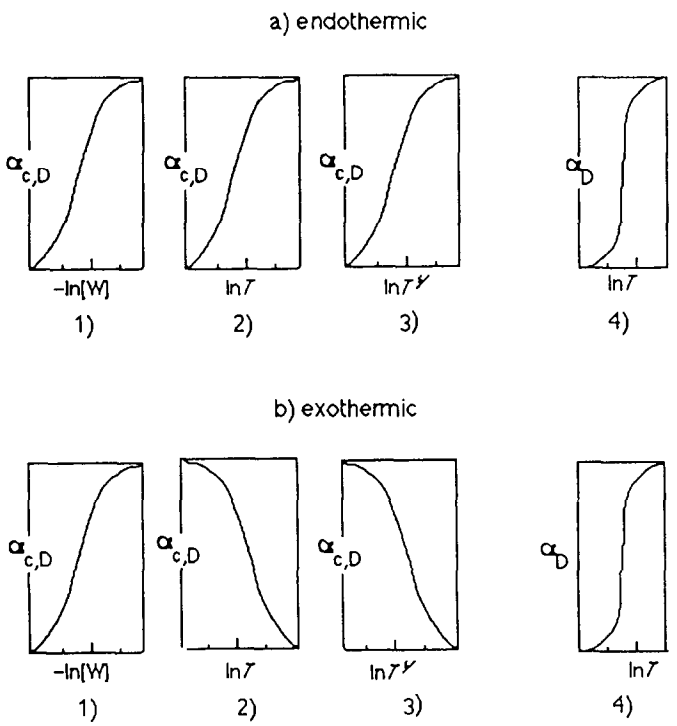

Fig. 5. Molar fraction and derivatives with respect to $-\ln[W]$, $\ln T$, and $\ln T^y$, respectively for (a) endothermic and (b) exothermic reaction. In any case, the resulting molar fraction change with the temperature is the same either in endo- or exothermic reactions.

In fact, in endothermic reactions, the "cold" molar fraction $\alpha_{c,D} = \partial \ln Z_N / \partial \ln[W]^{-n_W}$ (Fig. 5 (a, 1)) can be transformed into the "cold" derivative $(\partial \ln Z_N / \partial \ln[W]^{-n_W})/(\partial \ln[W]^{-n_W}/\partial \ln T)$ (Fig. 5(a, 2)) with $(\partial \ln[W]^{-n_W}/\partial \ln T) = +1$. In exothermic reactions, the "cold" derivative is reversed (Fig. 5(b, 2)) with $[\partial \ln[W]^{-n_W}/\partial \ln T) = -1$. The equality between "cold" derivatives is thus established

$$\partial \alpha_{c,D} / \partial \ln[W]^{-n_W} = \pm \alpha_{c,D} / \partial \ln T \tag{37}$$

where the plus sign holds for endothermic reactions and the minus sign for exothermic reactions.

By contrast, the "warm" molar fraction α_D can be calculated from eqn. (38)

$$\alpha_D = \kappa T^y / (1 + \kappa T^y) \tag{38}$$

This equation, if differentiated with respect to $\ln T^y$, produces the same slope as eqn. (37)

$$\partial \alpha_D / \partial \ln T^y = \pm \partial \alpha_{c,D} / \partial \ln T \tag{39}$$

where the plus sign holds for endothermic reactions (Fig. 5(a, 3)) and the minus sign for exothermic reactions (Fig. 5(b, 3)). (From eqn. (39) one obtains

$$y \partial \alpha_{c,D} / \partial \ln T = \pm \partial \alpha_D / \partial \ln T \tag{40}$$

where $y > 0$ and plus hold for endothermic reactions ((Fig. 5(a, 4)) and $y < 0$ and minus hold for endothermic reactions (Fig. 5(b, 4)). From the equality of the slopes of the diagrams in Fig. 5(a, 4) and 5(b, 4), one can deduce that endothermic and exothermic reactions give rise to corresponding buffer capacity curves. The right hand side eqn. (40) is equal to the left hand side eqn. (32).

The right hand side of eqn. (40) for an exothermic reaction can be introduced into eqn. (32) modified according to eqn. (37), to make the whole right hand side dependent upon the temperature

$$C_{p,app}/R = -\partial \alpha_D / \partial \ln T = (\partial \alpha_{c,D} / \partial \ln T)(\Delta H_0 / RT + n_W C_{p,W} / R) \tag{41}$$

This equation can be combined with eqn. (34) to show how $C_{p,app}$ is actually a mixed second moment of the distribution

$$C_{p,app}/R = (\partial \alpha_{c,D} / \partial \ln T)(\partial \ln[W]^{-n_W} / \partial \ln T) \tag{42}$$

obtained by double derivation, the former "cold" the latter "warm". Equation (42) confirms that the isobaric heat capacity is an evaluation of the dispersion of entropy due to both chemical and thermal dilution.

CALORIMETRIC DENATURATION ENTHALPY

The right hand side of eqn. (41) can be multiplied by R, transformed to the derivatives with respect to dT and integrated

$$\Delta H_{\text{den}} = \int_{T_1}^{T_2} C_{p,\text{app}}\, \mathrm{d}T$$

$$= (+\Delta H_0 + n_{\text{W}} C_{p,\text{W}} T_{\text{m}}) \int_{T_1}^{T_2} (\partial \alpha_{\text{c,D}}/\partial T)\, \mathrm{d}T \tag{43}$$

where T_1 and T_2 are the temperatures at which the transformation begins and ends, respectively. T_{m} is the temperature at which the buffer capacity is at a maximum and corresponds to the midpoint of the transformation. The result of the integration is

$$\Delta H_{\text{den}} = \Delta H_0 + n_{\text{W}} C_{p,\text{W}} T_{\text{m}} \tag{44}$$

which corresponds to eqn. (19) if T_{m} is substituted for T.

The value of the denaturation enthalpy, ΔH_{den} is usually calculated by integrating the area below the thermal profile between two temperatures and is equal to the total enthalpy of eqn. (44) (Fig. 6). This means that by plotting the apparent enthalpy ΔH_{den} measured at each temperature against T_{m}, one should obtain a straight line, in accordance also with eqn. (19) obtained for the equilibrium experiments performed at constant temperature. This result is in general found in many cases experimentally examined,

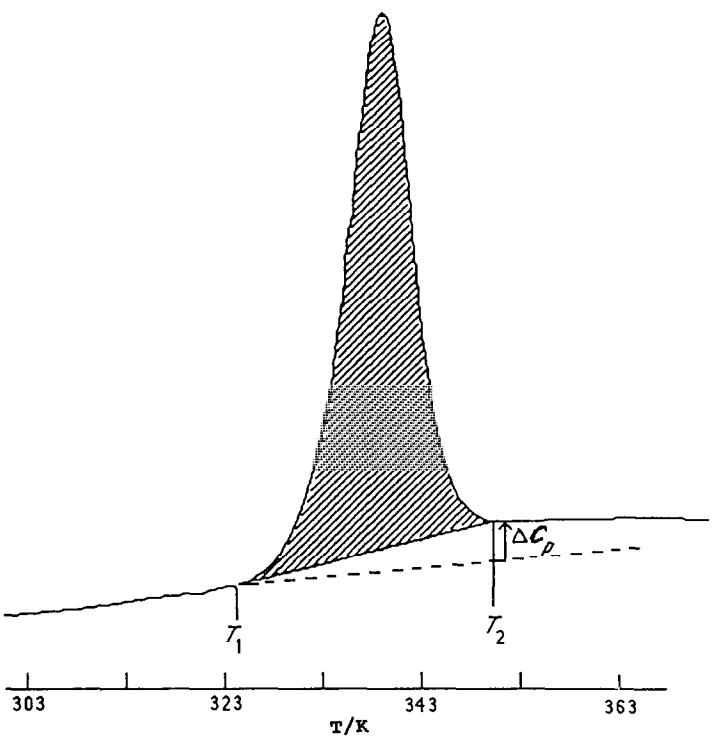

Fig. 6. Denaturation peak in DSC experiment.

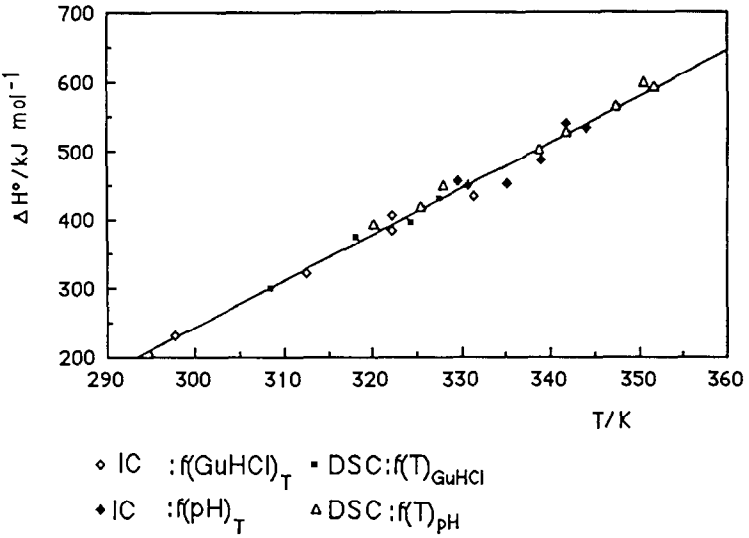

Fig. 7. Denaturation enthalpy of hen egg white lysozyme vs. temperature. IC, isothermal calorimetry; DSC, differential scanning calorimetry. Data from Privalov [16].

as is shown in the example of Fig. 7 where values obtained either by equilibrium or calorimetric experiments are plotted. This proves the validity of eqns. (19) and (44) for a two step denaturation process.

A possible molecular mechanism in accordance with the thermodynamic result is drawn in Fig. 8.

EFFECTS OF DENATURANT AND ACIDITY

The denaturation process occurs at different temperatures depending on the pH, and on the addition of denaturants. It has been found [15–20] that the enthalpy, ΔH_{den} at different temperatures (obtained by changing pH or denaturant concentration) plotted against the temperature T produces a straight line (see Fig. 7).

According to eqn. (36) the slope of the straight line is equal to $n_W C_{p,W}$ with $n_W = 89.9$ water molecules per mole in hen egg white lysozyme. The influence of the water molecules on the denaturation of proteins can be explained on the grounds of the previously mentioned equations. The contribution of the water molecules to the apparent isobaric heat capacity derives from eqn. (19) which is based on the equality between the entropy changes due to temperature and dilution. The slope $n_W C_{p,W}$ is therefore an entropy term ΔS_W

$$\Delta S_W = n_W C_{p,W} \tag{45}$$

The action of the denaturants, which are substances that produce at some concentration level the transition N → D can also be explained on the basis

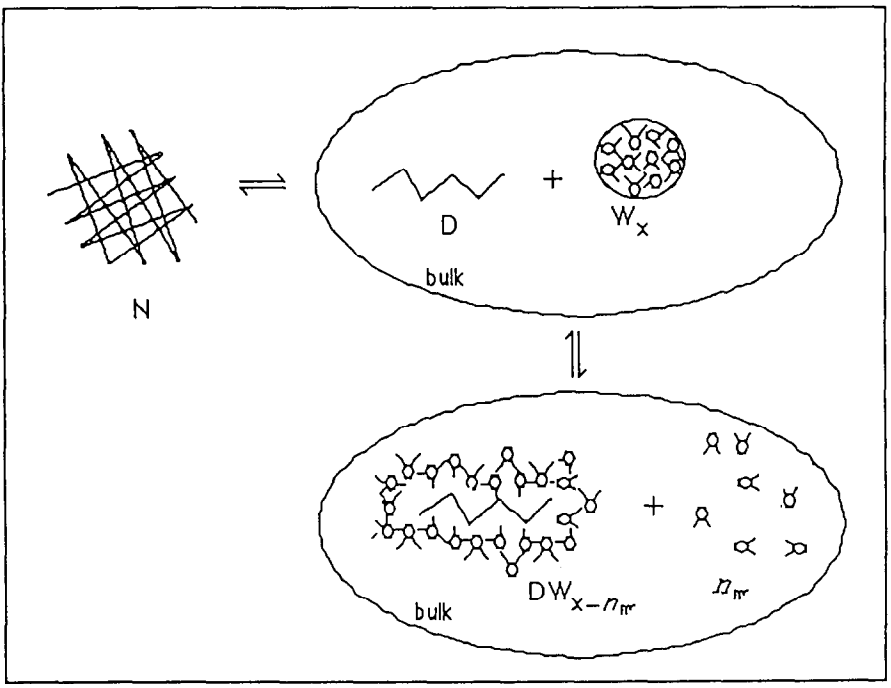

Fig. 8. Proposed molecular model of the denaturation process: N, native protein; D, denatured protein; DW_x, hydrated denatured protein; W_x: portion of bulk water; n_w, water molecules set free in the denaturation process.

of the model adopted here. The effect of denaturants upon denaturation has been analysed by Hade and Tanford [25], Lee and Timasheff [26] and by Schellman [27] amongst others.

One of the most active denaturants is guanidium chloride GuHCl. These substances could exert their action by subtracting water molecules from the sheath of the hydrophobic moiety. In such a way, the denaturants produce dilution of the water molecules of the sheath thus changing the dilution according to eqn. (19). In fact, one can write

$$\partial[\mathrm{W}]^{-n_\mathrm{W}}/\partial \ln T = \partial[\mathrm{W}]^{-n_\mathrm{W}}/\partial \ln[\mathrm{GuHCl}] = -[\mathrm{W}]^{-n_\mathrm{W}} n_\mathrm{W} C_{p,\mathrm{W}}/R \qquad (46)$$

which shows how a change of denaturant concentration is exactly equivalent to a change of the temperature. This is the reason why the points obtained by changing the concentration of denaturant at constant T fall on the same line as the points obtained at constant [GuHCl] by changing the temperature. The term ΔS_W is the one changing in eqns. (19) and (44).

On the same grounds, the effect of pH on the denaturation of proteins can be explained by putting the equality

$$\partial[\mathrm{W}]^{-n_\mathrm{W}}/\partial \ln T = \partial[\mathrm{W}]^{-n_\mathrm{W}}/\partial \mathrm{pH} = -[\mathrm{W}]^{-n_\mathrm{W}} n_\mathrm{W} C_{p,\mathrm{W}}/R \qquad (47)$$

and again the points obtained by changing the temperature at constant pH fall on the same line as the points obtained by changing pH at constant T. Again, the term ΔS_W is that which changes in eqns. (46) and (47).

Similar behaviour is presented by other macromolecules, e.g. by phenylalanine specific tRNA which has been studied as the function of temperature and Mg^{2+} concentration by Biltonen and co-workers [28, 29].

ANALYSIS OF EXPERIMENTAL DATA

The DSC microcalorimeter has been used by several authors [15–19] to study the equilibrium between native and denatured conformations of macromolecules.

The first set of data analysed in the light of the model proposed here is the set of data given by Privalov [16]; the calorimetric traces obtained for hen egg white lysozyme under different conditions of pH either by isothermal (IC) or differential scanning (DSC) calorimetry are shown in Fig. 9.

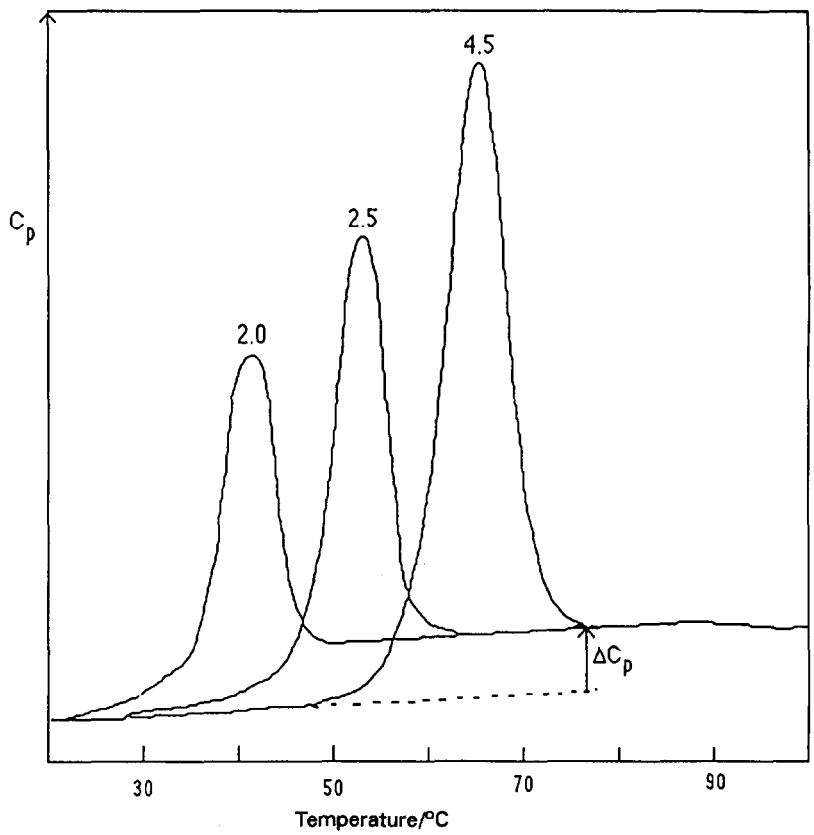

Fig. 9. DSC curves for the denaturation of a protein at different pH values. Reproduced from Privalov [16].

The values of the total enthalpy have been evaluated from the graph and are reported in Fig. 7. The number of water molecules obtained from the slope of the line in this diagram is $n_W = 88.9$.

Another set of data concerning various types of lysozyme has been obtained by Sturtevant [30]. The data refer to a wild type of lysozyme from bacteriophage T4 and its R96H and T157A mutants. The different types of lysozyme have been supplied to Professor Sturtevant by Brian Matthews of the University of Oregon. The wild T4 lysozyme has a sequence of 164 residues against 126 of hen egg white lysozyme. The molecular weight of T4 lysozyme is 18 700 Da against 14 100 Da for hen egg white lysozyme. The molecule of T4 lysozyme is larger than the molecule of hen egg white lysozyme and very probably presents a number of hydrophobic residues which is roughly proportional to the molecular size.

The data of the enthalpies for T4 lysozyme and its mutants are reported in Table 1. The temperatures listed are the temperatures of half completion of the transitions. Several different batches of proteins were used in each case and this could be the cause of the considerable scattering in the data. The temperature of denaturation was varied by varying the pH over the range 1.8 to 3.1.

The denaturation enthalpies are plotted against T in Fig. 10. The different mutants produce lines with different slopes corresponding to $n_W = 122$ (wild T4 lysozyme), $n_W = 131.4$ (for Thr157Ala), $n_W = 139.8$ (for Arg96His), respectively.

The changes in the number of water molecules n_W is coherent with the molecular features of the types of lysozyme (see Table 2). The variation between hen egg white and T4 lysozymes is related to the size of the molecules and is probably proportional to the number of hydrophobic residues. The changes of n_W between wild T4 lysozyme and its mutants are justified by the increased hydrophobic character of the substituents. Alanine is more hydrophobic than threonine and histidine more hydrophobic than arginine, respectively.

CONCLUSIONS

The enthalpy value ΔH^0 obtained by extrapolation of ΔH_{den} to $T = 0$ is the net enthalpy change of the reaction between protein and water. At $T = 0$, the water molecules released by the reaction do not absorb heat.

The extrapolated values, ΔH^0 for the different types of lysozyme are themselves a function of n_W (Fig. 11). The straight line

$$\Delta H^0 = \Delta h_a + \Delta h_W = +209 - 22.11 n_W \text{ kJ mol}^{-1} \quad (48)$$

fits the data. The enthalpy change $\Delta h_W = -22.11 n_W$ kJ per mol n_W is the enthalpy change per water molecule for the hydration of the protein while $\Delta h_a = +209$ kJ mol^{-1} is the conformational enthalpy change at denaturation.

TABLE 1

Calorimetric determination of denaturation enthalpy and denaturation temperature in wild T4 lysozyme and its mutants

T157A		R96H		Wild	
T/K	ΔH/kJ mol^{-1}	T/K	ΔH/kJ mol^{-1}	T/K	ΔH/kJ mol^{-1}
303.24	295.8	296.59	201.7	306.07	328.4
304.44	311.3	296.27	223.7	308.66	347.3
307.23	362.3	295.68	197.9	308.76	366.9
307.25	344.3	296.82	250.2	308.65	366.1
307.51	348.1	295.79	213.0	308.81	365.2
311.02	360.7	296.64	237.7	308.87	367.8
311.13	348.9	297.47	242.7	312.25	400.4
311.19	395.8	297.46	225.9	311.50	412.1
311.51	392.0	299.96	288.7	312.32	412.1
311.63	370.7	300.10	295.8	311.04	389.5
311.73	364.4	300.71	303.7	311.86	417.1
311.74	378.6	302.50	270.7	312.37	405.4
311.87	395.0	303.08	281.6	308.96	405.4
312.23	391.2	303.98	316.7	313.70	426.3
314.04	402.9	303.78	301.2	316.09	465.7
313.94	414.6	304.47	305.0	316.65	478.2
315.98	460.2	305.98	315.9	316.82	477.3
316.23	410.0	306.45	331.8	317.08	478.2
316.69	478.2	307.34	308.3	317.33	478.2
320.28	429.7	310.14	399.1	318.07	473.2
320.62	487.4	310.59	387.4	318.37	495.4
323.00	494.5	310.56	387.4	318.31	475.7
323.24	497.4	310.78	380.3	318.81	474.0
323.26	496.2	311.00	389.5	321.52	490.4
323.65	510.0	313.95	438.9	321.60	482.0
		314.23	409.2	321.80	488.3
		314.66	399.1	321.90	476.5
		314.46	399.1	322.05	463.2
				322.21	476.5
				324.91	516.3
				324.74	518.0

The term corresponding to the effect of the n_W water molecules can be represented as a vector $\Delta \boldsymbol{S}^{\ominus}_{W}$ in the thermodynamic space (Fig. A1). The free energy change is positive and the corresponding vector $\Delta \boldsymbol{G}^{\ominus}_{den}$ (Fig. A1(a)) is in the negative field, so is the denaturation (endothermic) enthalpy $\Delta \boldsymbol{H}_{den}$. The entropy component $\Delta \boldsymbol{S}^{\ominus}_{den}$ is positive.

$$\Delta \boldsymbol{G}^{\ominus}_{den} = \Delta \boldsymbol{H}_{den} + \Delta \boldsymbol{S}^{\ominus}_{den} \tag{49}$$

The enthalpy component can be decomposed into an endothermic vector, $\Delta \boldsymbol{H}_0$, which is in the positive field and a negative (endothermic) water

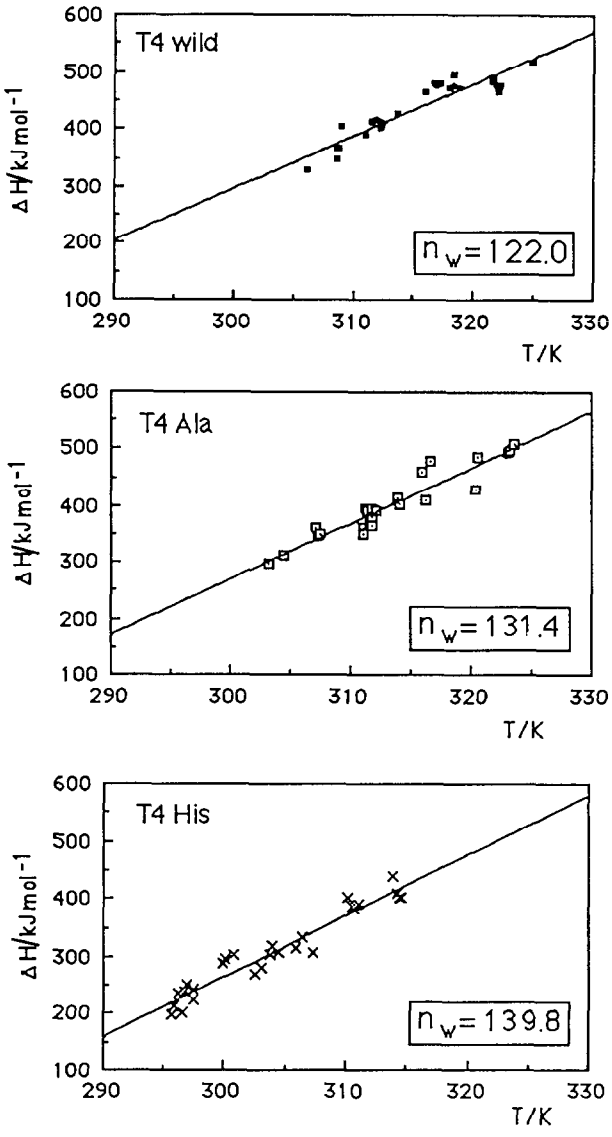

Fig. 10. Denaturation enthalpy as the function of absolute temperature T for different types of lysozyme obtained from bacteriophage T4. The mutants are T4 Ala = T157A and T4 His = R96H.

enthalpy, ΔH_W (Fig. A1(b)). In its turn ΔH_0 is the sum of the hydration (exothermic) enthalpy ΔH_{hyd} and of the endothermic conformational enthalpy ΔH_{conf}. The entropy component is the sum of the water entropy $\Delta S^{\ominus}_W$ of the conformational entropy ΔS_{conf} and of the hydration entropy $\Delta S^{\ominus}_{hyd}$ (Fig. A1(c))

$$\Delta G^{\ominus}_{den} = \Delta H_0 + \Delta H_W + \Delta S_{conf} + \Delta S^{\ominus}_W + \Delta S^{\ominus}$$
$$= -\Delta H_{hyd} + \Delta H_W + \Delta H_{conf} + \Delta S_{conf} + \Delta S^{\ominus}_W + \Delta S^{\ominus} \quad (50)$$

TABLE 2

Hydration numbers n_W of different types of lysozyme

Type	Slope/J mol^{-1} K^{-1}	n_W	ΔH^0/kJ mol^{-1}	T/K
HEW [a]	6701 [b]	88.9	−1764.8	263.4
Wild T4	9199 [c]	122	−2463.4	267.8
T157A (T4)	9903 [c]	131.4	−2701.7	272.8
R96H (T4)	10539 [c]	139.8	−2896.2	274.8

[a] Hen egg white. [b] Fig. 7. [c] Fig. 10.

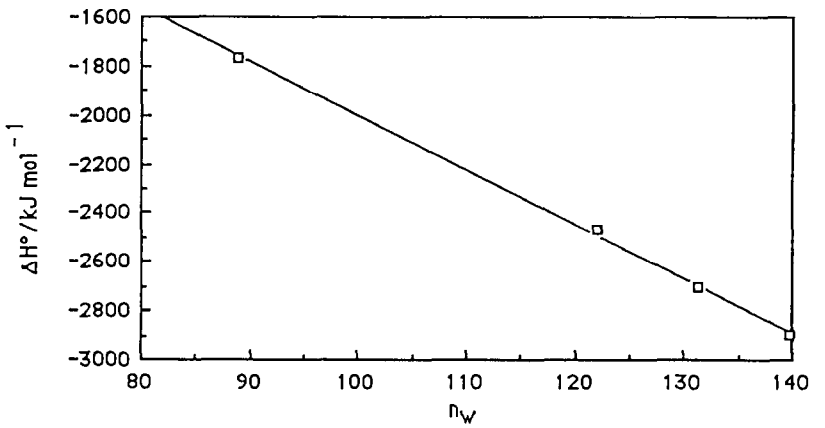

Fig. 11. The extrapolated enthalpy ΔH^0 for different types of lysozyme as the function of n_W (see eqn. (48)).

The combination of water enthalpy and of water entropy is null

$$\Delta \boldsymbol{H}_W + \Delta \boldsymbol{S}^{\ominus}_W = 0 \tag{51}$$

as is the combination of enthalpy and entropy for the conformational transition

$$\Delta \boldsymbol{H}_{conf} + \Delta \boldsymbol{S}_{conf} = 0 \tag{52}$$

and the denaturation free energy is the combination of

$$\Delta \boldsymbol{G}^{\ominus}_{den} = \Delta \boldsymbol{H}_{hyd} + \Delta \boldsymbol{S}^{\ominus}_{hyd} \tag{53}$$

Thus, the denaturation enthalpy can be decomposed into three contributions: (1) hydration of protein in a cavity in the solvent ΔH_{hyd}; (2) conformation enthalpy ΔH_{conf}; (3) heat absorbed by the water molecules released $n_W C_{p,A} T$. Contributions (2) and (3) are balanced by an opposing entropy contribution. Therefore, the resulting free energy charge for denaturation is small and mainly governed by entropy–enthalpy compensation.

ACKNOWLEDGEMENTS

Professor J.M. Sturtevant, Yale University, New Haven is warmly thanked for providing experimental data. The Italian Ministry for University and Scientific and Technological Research (MURST) and the Italian Research Council (CNR, Progetto finalizzato per la Chimica fine) are thanked for financial support.

REFERENCES

1 A. Braibanti, F. Dallavalle, G. Mori and M. Pasquali, Inorg. Chim. Acta, 91 (1984) 195.
2 A. Braibanti, F. Dallavalle, E. Fisicaro and M. Pasquali, Inorg. Chim. Acta, 122 (1986) 135.
3 A. Braibanti, E. Fisicaro, M. Monguidi and F. Dallavalle, Inorg. Chim. Acta, 138 (1987) 17.
4 A. Braibanti, F. Dallavalle and E. Fisicaro, Ann. Chim. (Rome), 78 (1988) 679.
5 A. Braibanti, F. Dallavalle and E. Fisicaro, Thermochim. Acta, 140 (1989) 203.
6 E. Fisicaro, A. Braibanti, J.D. Lamb and J.L. Oscarson, Biophys. Chem., 36 (1990) 1.
7 E. Fisicaro, A. Braibanti, J.D. Lamb and J.L. Oscarson, Biophys. Chem., 36 (1990) 15.
8 E. Fisicaro, A. Braibanti, J.D. Lamb and J.L. Oscarson, Thermochim. Acta, 168 (1990) 161.
9 A. Braibanti, E. Fisicaro, F. Dallavalle and F.X. Ughi, Ann. Chim. (Rome), 80 (1990) 303.
10 A. Braibanti, E. Fisicaro, F. Dallavalle, J.D. Lamb and J.L. Oscarson, J. Phys. Chem., 97 (1993) 8054.
11 A. Braibanti, E. Fisicaro, F. Dallavalle, J.D. Lamb and J.L. Oscarson, J. Phys. Chem., 97 (1993) 8062.
12 A. Braibanti, E. Fisicaro, F. Dallavalle, J.D. Lamb, J.L. Oscarson and F.X. Ughi, J. Phys. Chem., 97 (1993) 8071.
13 A. Braibanti, E. Fisicaro, F. Dallavalle, J.D. Lamb, J.L. Oscarson and R. Sambasiva Rao, J. Phys. Chem., 98 (1994) 626.
14 A. Braibanti, Pure App. Chem., in press.
15 W. Pfeil and P.L. Privalov, Biophys. Chem., 4 (1976) 23.
16 P.L. Privalov, Pure Appl. Chem., 47 (1976) 293.
17 J.M. Sturtevant, Annu. Rev. Phys. Chem., 38 (1987) 463.
18 P.L. Privalov and S.J. Gill, Adv. Protein Chem., 39 (1988) 191.
19 P. Privalov, Annu. Rev. Biophys. Biophys. Chem., 18 (1989) 47.
20 M.M. Santoro, Y. Liu, S.M.A. Khem., L.-X. How and D.W. Bolen, Biochemistry, 31 (1992) 5278.
21 J.F. Brandts and L. Hunt, J. Am. Chem. Soc., 89 (1967) 4826.
22 J.F. Brandts, J. Am. Chem. Soc., 86 (1964) 4291.
23 J.F. Brandts, J. Am. Chem. Soc., 86 (1964) 4302.
24 D. Poland, Cooperative Equilibria in Physical Biochemistry, Clarendon, Oxford, 1978.
25 E.P.K. Hade and C. Tanford, J. Am. Chem. Soc., 89 (1957) 5034.
26 J.C. Lee and S.N. Timasheff, Biochemistry, 13 (1974) 257.
27 J.A. Schellman, Biophys. Chem., 45 (1993) 273.
28 J. Levy, G. Rialdi and R. Biltonen, Biochemistry, 11 (1972) 4907.
29 J. Levy and R. Biltonen, Biochemistry, 11 (1972) 4175.
30 J.M. Sturtevant, personal communication, 1993.

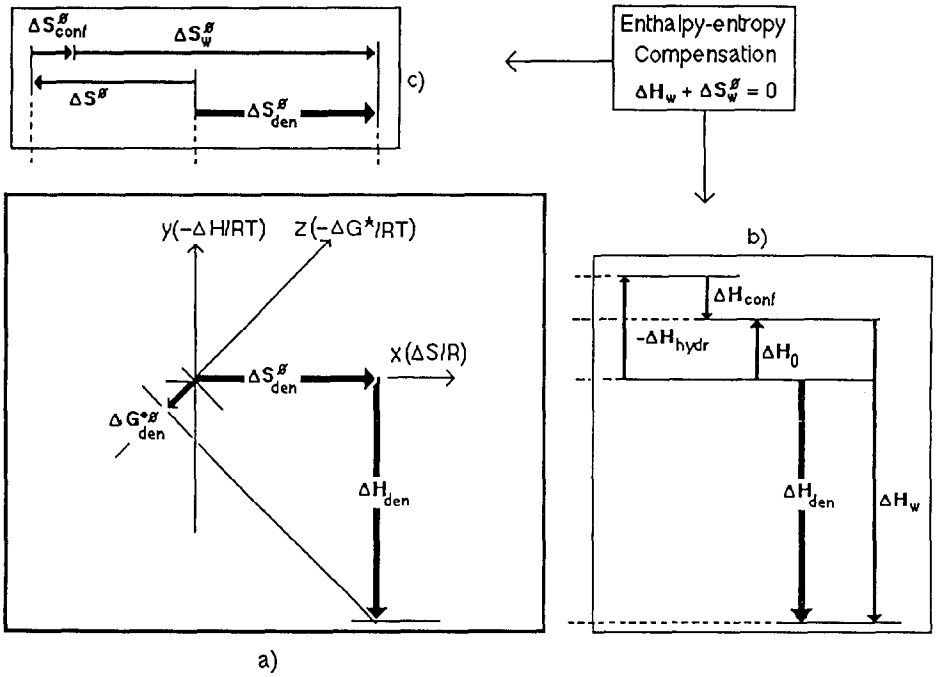

Fig. A1. Vector representation of the denaturation process.

APPENDIX: VECTORS IN THERMODYNAMIC AFFINITY SPACE AND IN THERMODYNAMIC FREE ENERGY SPACE (Fig. A1)

We define three coplanar vectors

$$x\boldsymbol{i} + y\boldsymbol{j} = z\boldsymbol{k}^* \tag{A1}$$

where $\boldsymbol{i}, \boldsymbol{j}, \boldsymbol{k}^*$ are unitary vectors of moduli $|\boldsymbol{i}| = 1/R$, $|\boldsymbol{j}| = 1/(RT)$, $|\boldsymbol{k}^*| = 0.707/(RT)$, respectively. $\boldsymbol{k}^*$ is the bisector of the angle between $\boldsymbol{i}$ and $\boldsymbol{j}$. If we substitute ΔS, $-\Delta H$, and $-\Delta G$ for x, y, z, respectively, we obtain

$$\Delta S\boldsymbol{i} + (-\Delta H)\boldsymbol{j} = (-\Delta G)\boldsymbol{k}^* \tag{A2}$$

which becomes in vector notation, in thermodynamic affinity space

$$\Delta \boldsymbol{S} - \Delta \boldsymbol{H} = -\Delta \boldsymbol{G}^* \tag{A3}$$

Note that $y\boldsymbol{j} = (-\Delta H)\boldsymbol{j} = -\Delta \boldsymbol{H}$ (exothermic reaction) and the vector $-\Delta \boldsymbol{H}$ is in the positive field ($y > 0$) in thermodynamic affinity space whereas $-y\boldsymbol{j} = (\Delta H)\boldsymbol{j} = \Delta \boldsymbol{H}$ (endothermic reactions), and the vector $\Delta \boldsymbol{H}$ is in the negative field ($y < 0$). The same rules hold for exoergonic reactions ($-\Delta \boldsymbol{G}$) in the positive field ($z^* > 0$) and endoergonic reactions ($\Delta \boldsymbol{G}$) in the negative field ($z^* < 0$), respectively.

Alternatively, in thermodynamic free energy space we substitute ΔS, ΔH, and ΔG for x, y, z, respectively, and obtain

$$\Delta S\boldsymbol{i} = \Delta H\boldsymbol{j} = \Delta G\boldsymbol{k}^* \tag{A4}$$

The vector $\Delta H\boldsymbol{j} = \Delta \boldsymbol{H}$ is in the positive upper field for endothermic reactions and the vector $-\Delta H\boldsymbol{j} = -\Delta \boldsymbol{H}$ is in the negative lower field for exothermic reactions. Analogously, the vector $\Delta G\boldsymbol{k}^* = \Delta \boldsymbol{G}$ is in the positive ($z^* > 0$) field for endoergonic reactions and the vector $-\Delta G\boldsymbol{k}^* = -\Delta \boldsymbol{G}$ is in the negative ($z^* < 0$) field for exoergonic reactions.

The thermodynamic affinity space is parallel to the probability space for transitions, whereas the thermodynamic free energy space is symmetrical to the probability space for transitions.